

Formation of Cubic Ice via Clathrate Hydrate, Prepared in Ultrahigh Vacuum under Cryogenic Conditions

Jyotirmoy Ghosh,[†] Radha Gobinda Bhui,^{†,‡} Gaurav Vishwakarma,[†] and Thalappil

*Pradeep^{†, *}*

[†]DST Unit of Nanoscience (DST UNS) and Thematic Unit of Excellence (TUE), Department of Chemistry, Indian Institute of Technology Madras, Chennai 600036, India

[‡]Present Address: Lehrstuhl für Physikalische Chemie II, Friedrich-Alexander-Universität Erlangen-Nürnberg, Egerlandstr. 3, 91058 Erlangen, Germany

Corresponding Author

*To whom correspondence should be addressed, E-mail: pradeep@iitm.ac.in

Table of contents

Name	Description	Page number
	Experimental section	S3-S5
Figure S1	Isothermal time-dependent RAIR spectra of 150 MLs of pure acetone film at 115, 120, and 125 K.	S6
Figure S2	Temperature-dependent RAIR spectra of 300 MLs acetone:H ₂ O (1:1).	S7
Figure S3	Temperature-dependent RAIR spectra of 300 MLs acetone:H ₂ O (1:20).	S8

Figure S4	Time-dependent RAIR spectra of 300 MLs of acetone:H ₂ O for two different ratios; (1:10) and (1:20)	S9
Figure S5	Time-dependent RAIR spectra of 300 MLs of acetone:H ₂ O (1:1) at 130 K.	S10
Figure S6	Time-dependent RAIR spectra of 300 MLs of acetone:H ₂ O (1:1) at 120 K.	S11
Figure S7	Time-dependent RAIR spectra of 300 MLs of acetone:D ₂ O (1:1) at 140 K.	S12
Figure S8	Time-dependent RAIR spectra of 150 MLs of solid H ₂ O film at 120 K, and 130 K.	S13
Figure S9	TPD-MS spectra of 150 MLs of pure acetone.	S14
Figure S10	Deconvoluted desorption trace of acetone, taken from the TPD spectra shown in Figure 3a of the main manuscript.	S15
Figure S11	Time-dependent RAIR spectra of 300 MLs of acetone:HDO (5% D ₂ O in H ₂ O) at 130 K.	S16
Figure S12	Time-dependent RAIR spectra of 300 MLs of acetone:HDO (5% D ₂ O in H ₂ O) at 132 K.	S17
Figure S13	Time-dependent RAIR spectra of 300 MLs of acetone:HDO (5% D ₂ O in H ₂ O) at 135 K.	S18
Figure S14	Time-dependent RAIR spectra of 300 MLs of acetone:HDO (5% D ₂ O in H ₂ O) at 137 K.	S19
Figure S15	Crystallization fractions of 300 MLs of acetone:HDO (5% D ₂ O in H ₂ O) at 130, 132, 135, and 137 K.	S20
Table S1	Different crystallization parameters of Ice I _c at 130, 132, 135, and 137 K.	S21
Figure S16	Plot of $\ln(-\ln[1-x(t)])$ vs. $\ln(t)$ at 130, 132, 135, and 137 K.	S22

Experimental Section:

Experiments were carried in an ultrahigh vacuum (UHV) chamber (base pressure $\sim 5 \times 10^{-10}$ mbar). Details of the instrument are described elsewhere.¹ This kind of low pressure is an essential condition for simulating the ISM or cometary environments. The vacuum was maintained by several oil-free turbomolecular pumps backed by diaphragm pumps (Pfeiffer Vacuum). In brief, the chamber was equipped with reflection absorption infrared (RAIR) spectroscopy and temperature-programmed desorption (TPD) mass spectrometry. Here, a Ru(0001) single crystal was used as the substrate. A thin film of ice was grown on top of this substrate, mounted on a copper holder, which in turn, was attached at the tip of a closed cycle helium cryostat (ColdEdge Technologies). The temperature was measured by using a K-type thermocouple connected to it. Repeated heating at 400 K before vapor deposition ensured surface cleanliness. The temperature ramping was controlled and monitored by a temperature controller (Lakeshore 336).

Acetone hydrate was formed by using $\sim 99.99\%$ pure acetone, purchased from Sigma-Aldrich and Millipore water (H_2O of $18.2 \text{ M}\Omega$ resistivity), taken in separate test tubes, connected to the sample line through a glass-to-metal seal. Here, both acetone and water were additionally purified through several freeze-pump-thaw cycles before introduction into the experimental chamber. The sample lines were connected to the experimental chamber through a high precision all-metal leak valve. These leak valves were used to control the flow or inlet pressure of different samples. Out of the two sample inlet lines, one was exclusively used for acetone while the other line was used for water deposition. During the exposure of different samples into the UHV chamber, their purities were checked using a quadrupole mass spectrometer (Extrel) installed in the chamber. Recorded mass spectra were used to monitor purity as well as to measure the ratio of the mixtures. The ratio of the mixed ice was determined by controlling the flow or inlet pressure of the sample. Here, we express the film thickness in terms of the monolayer (ML), assuming that $1.33 \times 10^{-6} \text{ mbar}\cdot\text{s} = 1 \text{ ML}$ which has been estimated to contain $\sim 1.1 \times 10^{15} \text{ molecules}\cdot\text{cm}^{-2}$. A number of reports²⁻⁴ adopted this calculation for the estimation of surface coverages. The inlet pressure during sample deposition was decided based on the coverage desired at the time of the experiment. The substrate was kept in a fixed perpendicular position for uniform growth of ice. For accurate estimations, the relative sensitivities of ion gauge response (ion gauge coefficient) towards different molecules have to be accounted.⁵ Other ways of estimating coverage include determination of molecular flux by Hertz-Knudsen equation, numerical integration of thermal desorption spectra.⁶ Despite this limitation, the

present method was chosen for its simplicity. A 1:1 monolayer mixture of acetone:H₂O will be 3.22:1 in molar ratio. However, it is difficult to estimate the actual ratio (acetone:H₂O) during the nucleation of acetone hydrate at higher temperature, due to the desorption of acetone. The nucleation is primarily governed by the annealing temperature and residence time. Therefore, the accurate measurement of the ratio of the mixture is insignificant for this study.

Here, to prepare 300 MLs of acetone:H₂O (1:1), the UHV chamber was backfilled at a total pressure of $\sim 5 \times 10^{-7}$ mbar (where, acetone inlet pressure = 2.5×10^{-7} mbar, and water inlet pressure = 2.5×10^{-7} mbar) and deposition was continued for 10 minutes. Now, this mixed ice was slowly (heating rate = 2 K.min⁻¹) heated to the required experimental temperatures (120, 130, and 135 K). At these temperatures, the mixed ice was monitored constantly by RAIRS with time. For decoupled O-D stretching analysis, the samples were prepared using D₂O ($\sim 5\%$) in H₂O.⁷ In this solution, D₂O undergoes H/D exchange to form HDO. The use of HDO facilitates the observation of ASW crystallization because the O-D stretching vibration is decoupled from intramolecular and intermolecular O-H stretching vibrations.⁷⁻⁹

RAIR spectra were recorded using a Bruker FT-IR spectrometer, Vertex 70. The external IR beam was focused onto the substrate using gold plated mirrors through ZnSe flanges (transparent to IR beam), attached to the vacuum chamber. The reflected IR beam from the substrate was re-focused using another gold-plated mirror to a liquid N₂ cooled external MCT IR detector. The spectra were collected in the 4000-550 cm⁻¹ range with 2 cm⁻¹ resolution. Each spectrum was averaged for 512 scans to get a better signal to noise ratio.

The CHs produced in the UHV condition were further characterized by temperature programmed desorption-mass spectrometry (TPD-MS) analysis. For TPD-MS, after ice deposition or clathrate hydrate formation, the substrate was moved to a fixed position by using a sample manipulator to ensure that the surface is very close to the mass spectrometer inlet and the substrate was ramped at a constant heating rate (30 K.min⁻¹). Suitable masses of the desorbed species ($m/z = 43$ for acetone, $m/z = 18$ for H₂O) were selected by a linear quadrupole mass spectrometer analyzer, and the intensity of the desorbed species was plotted as a function of substrate temperature. Extrel CMS, USA supplied the mass spectrometers.

Reflection high-energy electron diffraction (RHEED) study was carried out in a different UHV chamber of base pressure $\sim 1.33 \times 10^{-10}$ mbar, which was described in detail elsewhere.¹⁰ To obtain RHEED patterns, we used a focused high-energy electron beam (30 keV) that was generated by an electron gun (Eiko Co. Ltd., MB-1000). The diffraction pattern projected onto a phosphor screen was recorded using a high-sensitivity CCD camera intermittently (pulse duration of ~ 0.5 s), only at specific temperatures and coverages of interest to reduce sample

damage. The typical electron beam current during the RHEED measurement was 5-7 nA, as determined using a Faraday cup. The spot size and glancing angle of the beam were 0.1 mm and 2-3°, respectively.

Supporting Information 1:

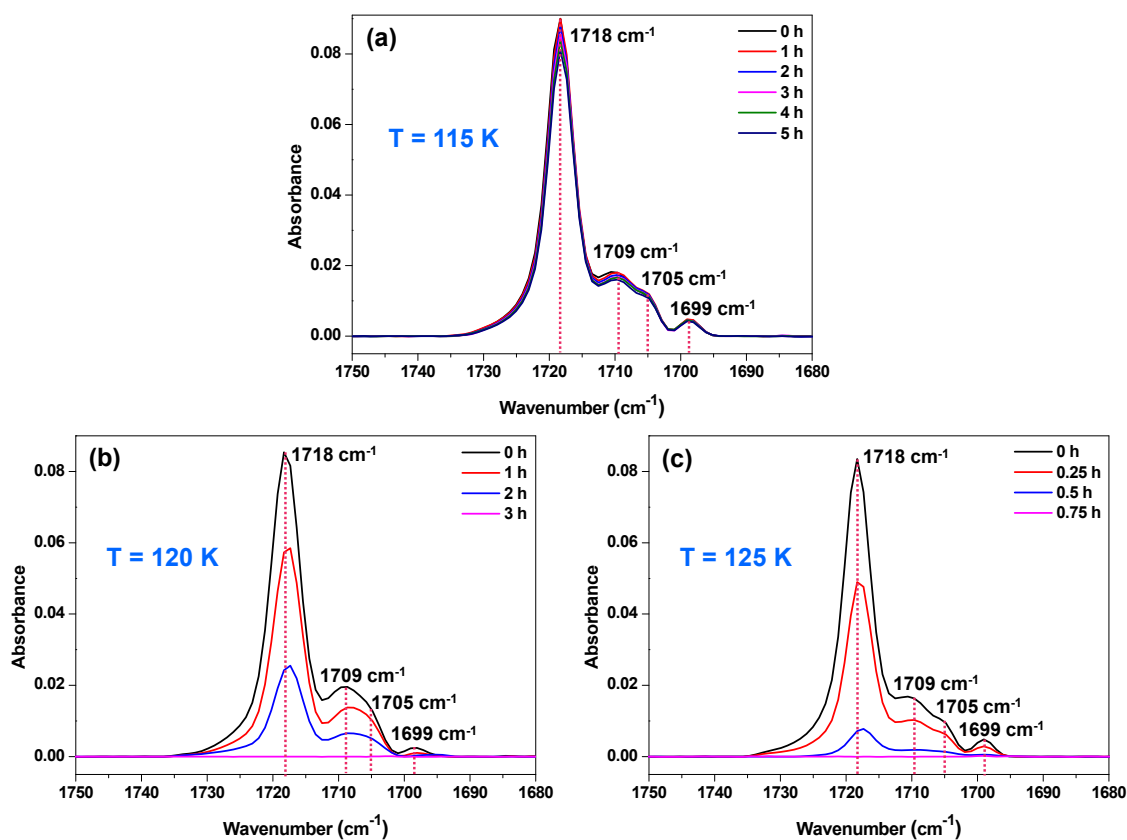


Figure S1. Isothermal time-dependent RAIR spectra of 150 MLs of pure acetone film at (a) 115, (b) 120, and (c) 125 K in the C=O stretching region. Time-dependent studies at relatively higher temperatures (130 or 135 K) could not be performed, since pure acetone desorbs within a few minutes at these temperatures.

Supporting Information 2:

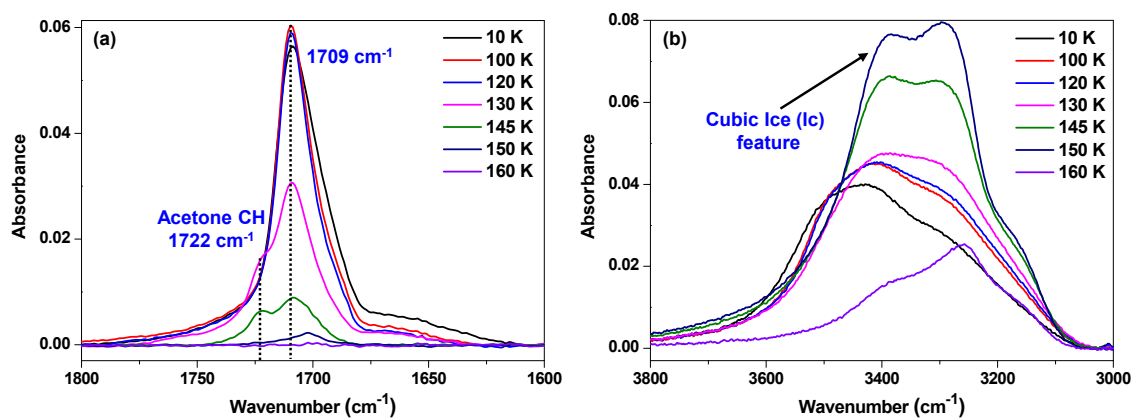


Figure S2. Temperature-dependent RAIR spectra of 300 MLs acetone:H₂O (1:1) in the (a) C=O stretching region, and (b) O-H stretching region. The mixture was co-deposited on Ru(0001) substrate at 10 K, and annealed at a rate of 2 K.min⁻¹.

Supporting Information 3:

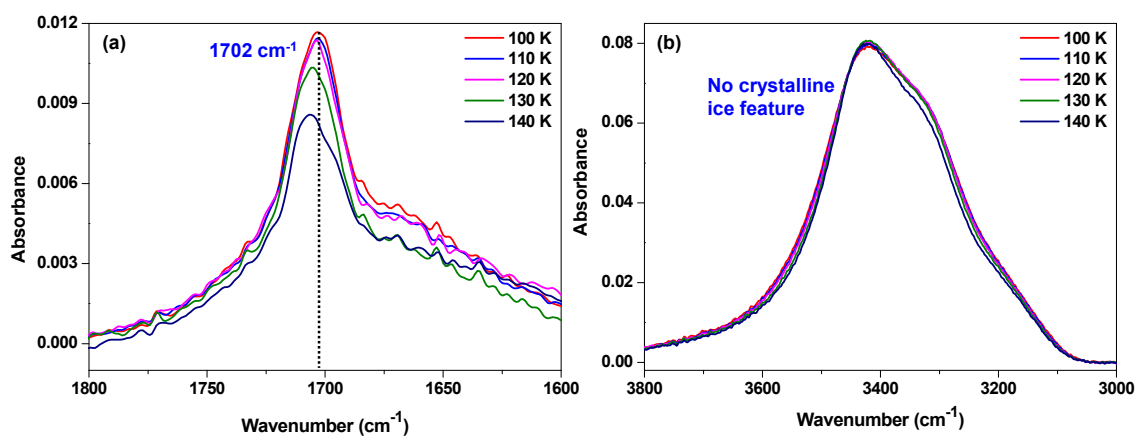


Figure S3. Temperature-dependent RAIR spectra of 300 MLs acetone:H₂O (1:20) in the (a) C=O stretching region, and (b) O-H stretching region. The mixture was co-deposited on Ru(0001) substrate at 10 K, and annealed at a rate of 2 K.min⁻¹ to 140 K. The C=O stretching region partly overlaps with the O-H bending feature. Noise in the spectra is due to the reduced concentration of acetone.

Supporting Information 4:

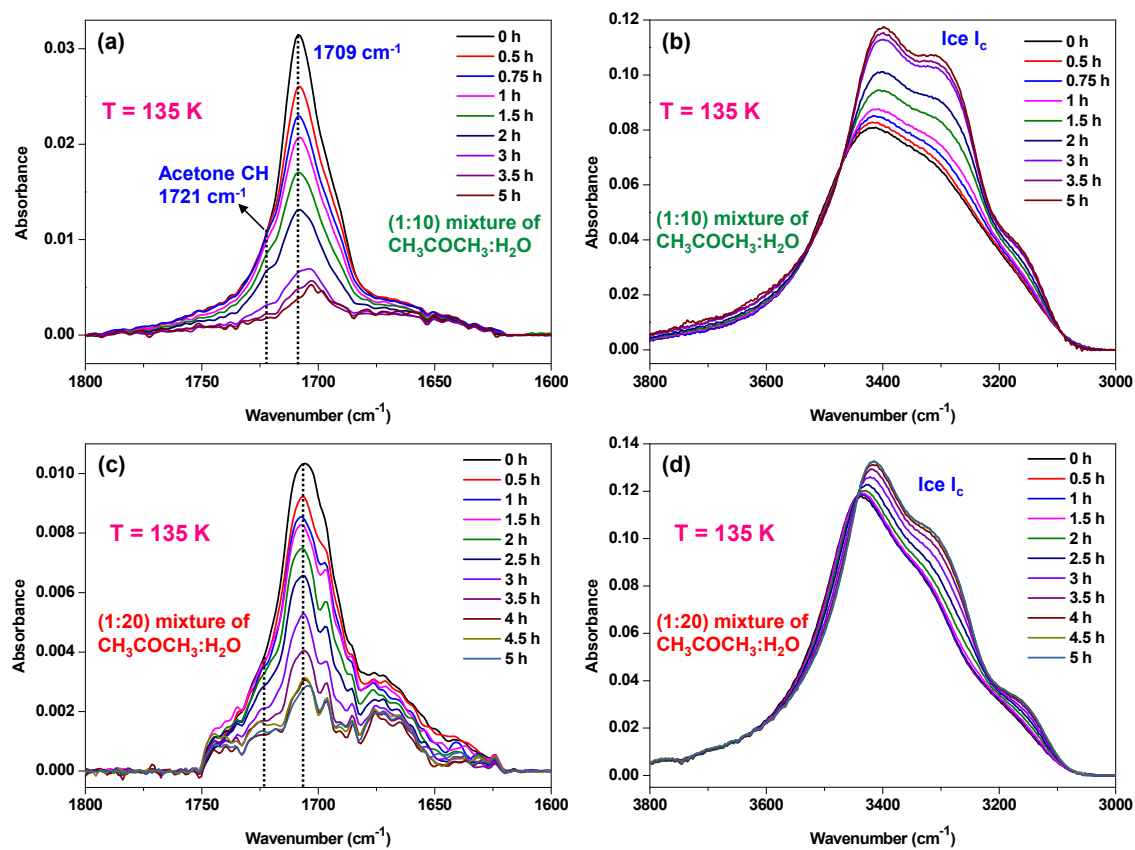


Figure S4. Time-dependent RAIR spectra of 300 MLs of acetone:H₂O for two different ratios; (1:10) and (1:20) as shown in the top and bottom panels, respectively.

Supporting Information 5:

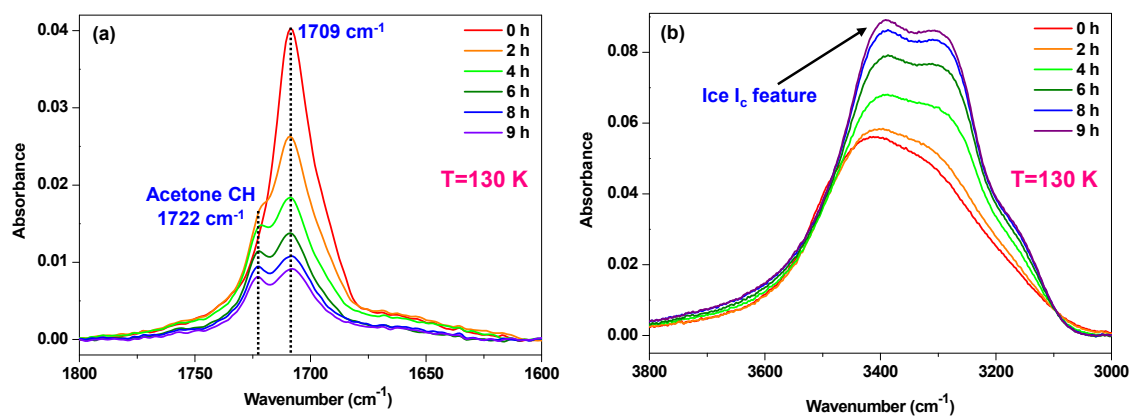


Figure S5. Time-dependent RAIR spectra of 300 MLs of acetone:H₂O (1:1) at 130 K in the (a) C=O stretching region, and (b) O-H stretching region. The mixture was co-deposited on Ru(0001) substrate at 10 K, and annealed at a rate of 2 K.min⁻¹ to 130 K.

Supporting Information 6:

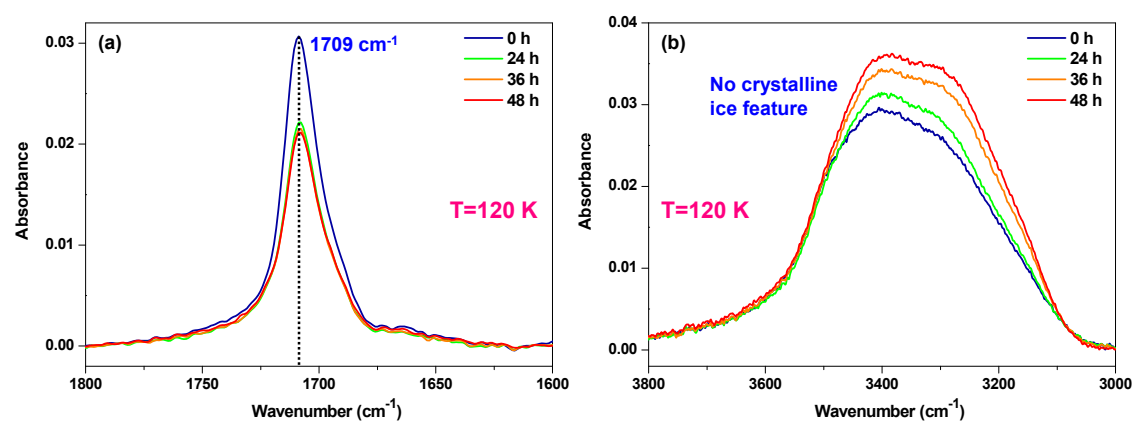


Figure S6. Time-dependent RAIR spectra of 300 MLs of acetone:H₂O (1:1) at 120 K in the (a) C=O stretching region, and (b) O-H stretching region. The mixture was co-deposited on Ru(0001) substrate at 10 K, and annealed at a rate of 2 K.min⁻¹ to 120 K.

Supporting Information 7:

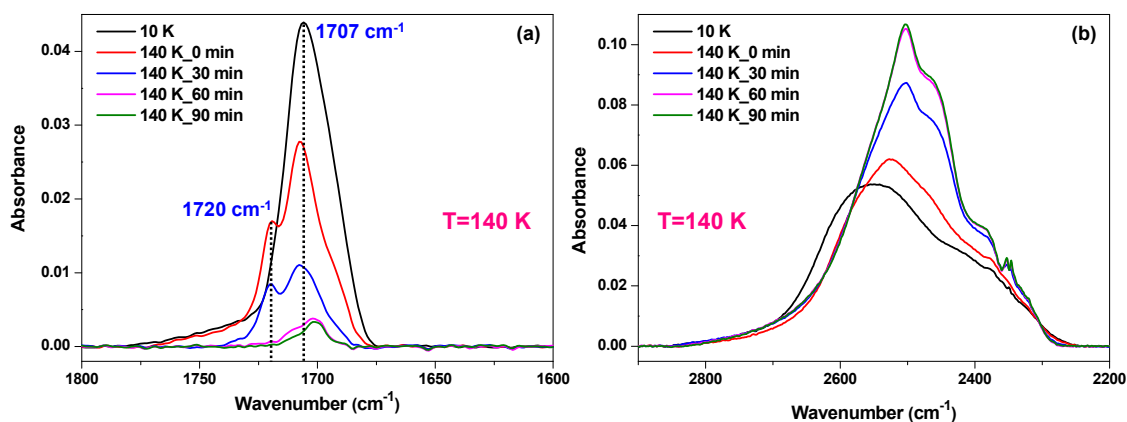


Figure S7. Time-dependent RAIR spectra of 300 MLs of acetone:D₂O (1:1) at 140 K in the (a) C=O stretching region, and (b) O-D stretching region. The mixture was co-deposited on Ru(0001) substrate at 10 K, and annealed at a rate of 2 K.min⁻¹ to 140 K. The small peak at ~2349 cm⁻¹ is due to the uncompensated gas phase CO₂ from the background.

Supporting Information 8:

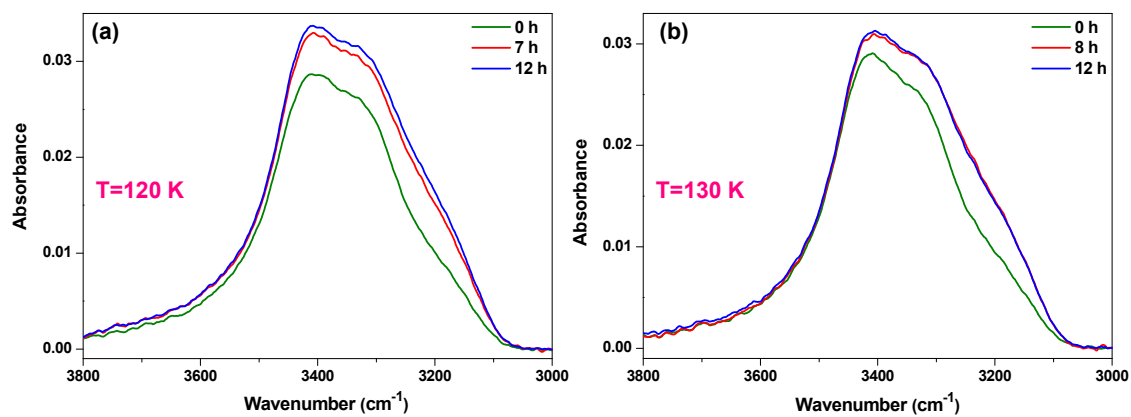


Figure S8. Time-dependent RAIR spectra of 150 MLs of solid H₂O film at (a) 120 K, and (b) at 130 K in the O-H stretching region. The water vapour was deposited at 10 K on Ru(0001) substrate. The ice films were annealed at 2 K.min⁻¹ rate to the respective temperatures.

Supporting Information 9:

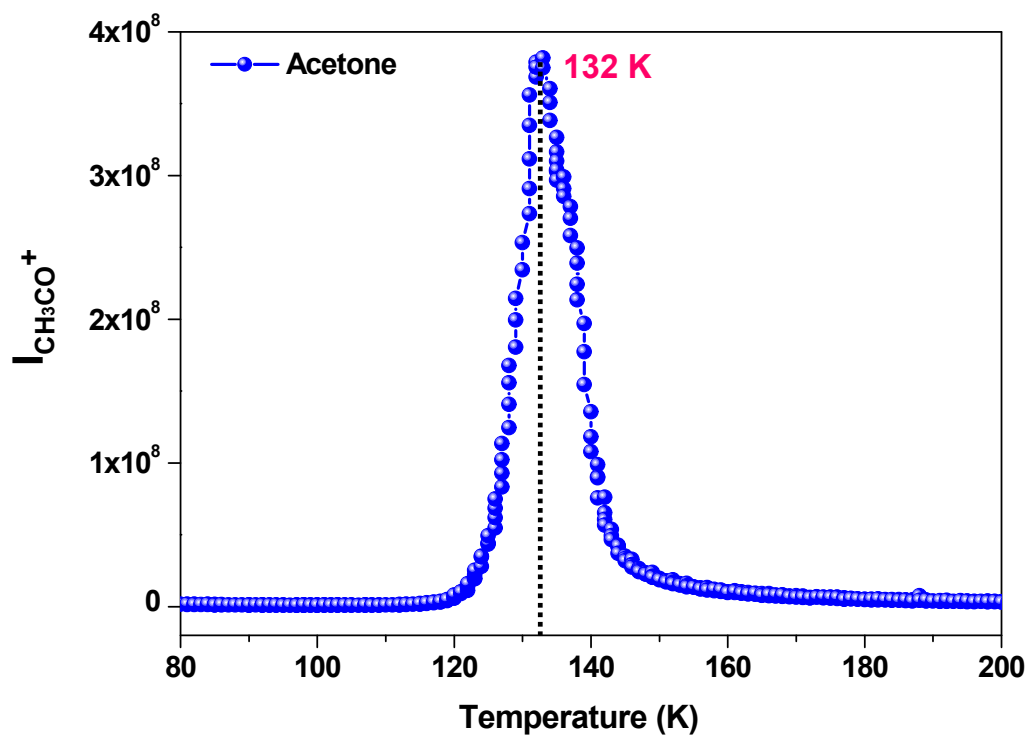


Figure S9. TPD-MS spectra of 150 MLs of pure acetone. Ramping rate = 30 K.min⁻¹.

Supporting Information 10:

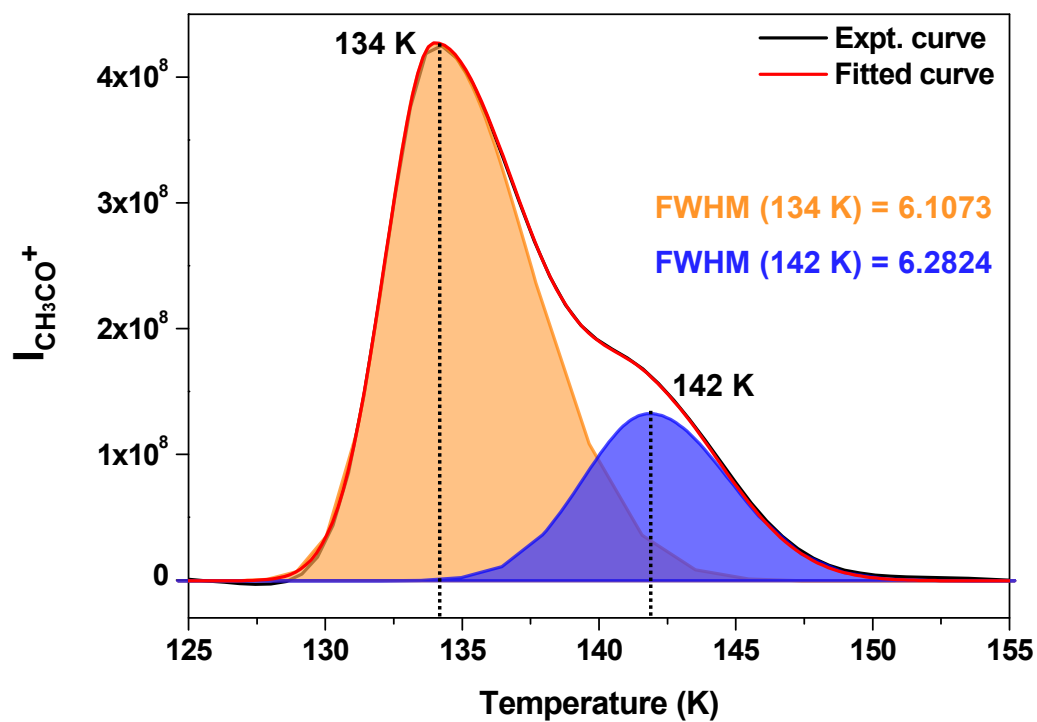


Figure S10. Deconvoluted desorption trace of acetone, taken from the TPD spectra shown in Figure 3a of the main manuscript. Here, two components are fitted to show their spectral widths are almost the same.

Supporting Information 11:

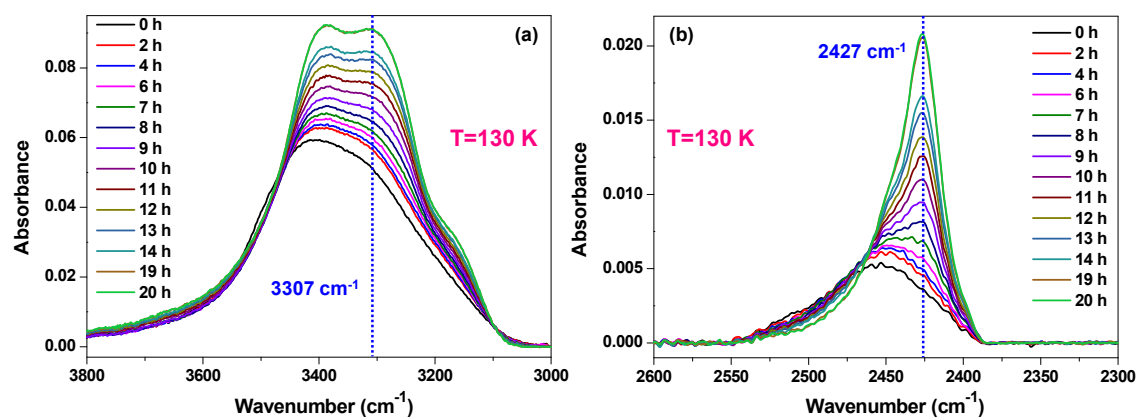


Figure S11. Time-dependent RAIR spectra of 300 MLs of acetone:HDO (5% D_2O in H_2O) at 130 K in the (a) O-H stretching region, and (b) O-D stretching region.

Supporting Information 12:

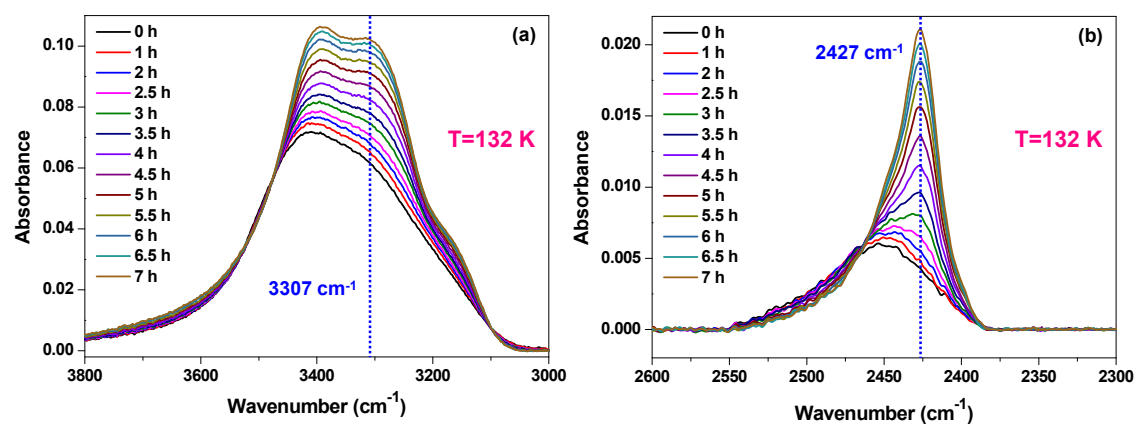


Figure S12. Time-dependent RAIR spectra of 300 MLs of acetone:HDO (5% D_2O in H_2O) at 132 K in the (a) O-H stretching region, and (b) O-D stretching region.

Supporting Information 13:

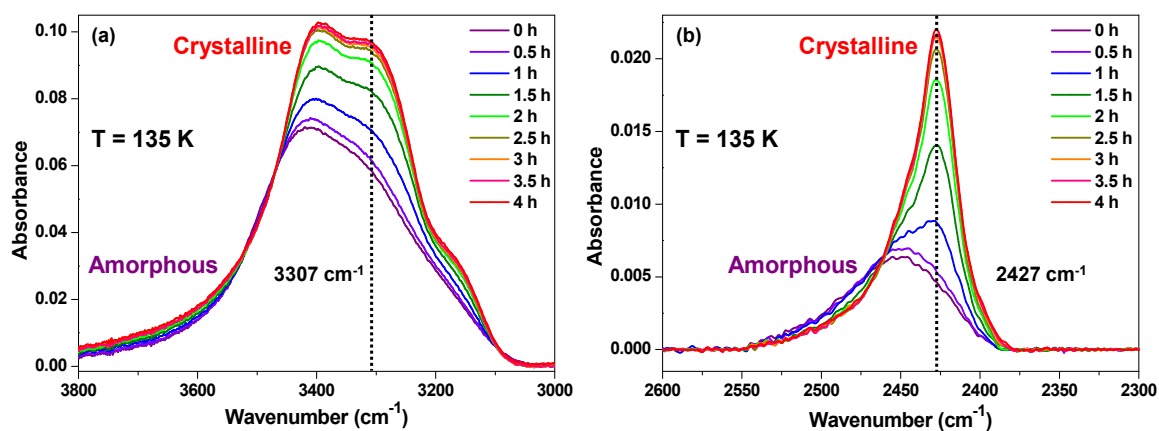


Figure S13. Time-dependent RAIR spectra of 300 MLs of acetone:HDO (5% D_2O in H_2O) at 135 K in the (a) O-H stretching region, and (b) O-D stretching region. The mixture was co-deposited on Ru(0001) substrate at 10 K, and annealed at a rate of $2 \text{ K}\cdot\text{min}^{-1}$ to 135 K. The vertical lines at a fixed wavenumber are used to measure the absorbance changes with time, which was further utilized for calculation of crystallization fraction.

Supporting Information 14:

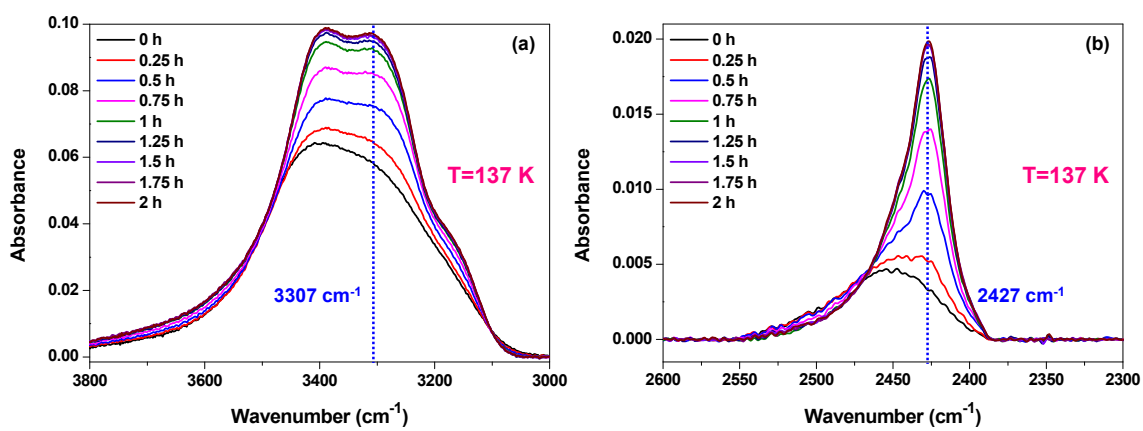


Figure S14. Time-dependent RAIR spectra of 300 MLs of acetone:HDO (5% D₂O in H₂O) at 137 K in the (a) O-H stretching region, and (b) O-D stretching region.

Supporting Information 15:

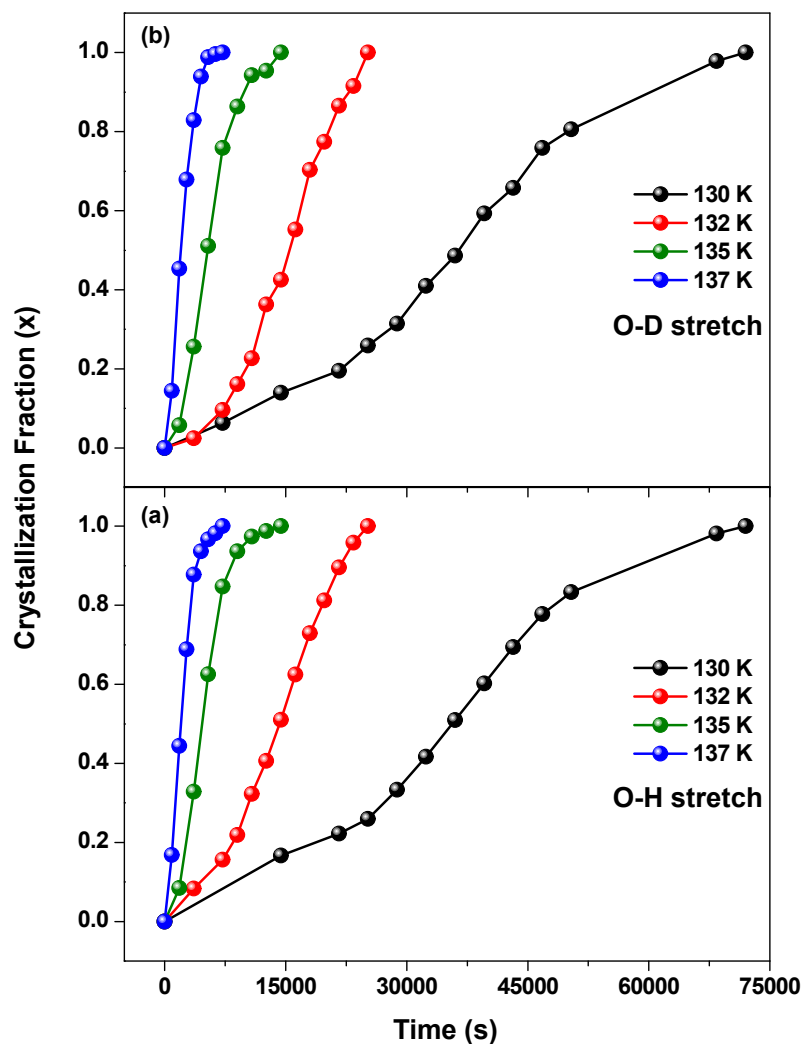


Figure S15. Crystallization fraction of 300 MLs of acetone:HDO (5% D₂O in H₂O) obtained from isothermal RAIRS measurements at 130, 132, 135, and 137 K. The extent of crystallization were estimated from, (a) the 3307 cm⁻¹ peak in the O-H stretching region, and (b) the 2427 cm⁻¹ peak in the decoupled O-D stretching region.

Table S1: The parameters for crystallization of ice Ic during the dissociation of acetone hydrate at different temperatures.

	Temperature (K)	n	Rate constant; k (s ⁻¹)
O-H stretching	130	2.49	2.47×10^{-5}
	132	2.45	6.37×10^{-5}
	135	2.05	1.80×10^{-4}
	137	1.62	4.04×10^{-4}
O-D stretching	130	2.59	2.36×10^{-5}
	132	2.51	5.76×10^{-5}
	135	2.08	1.50×10^{-4}
	137	1.81	3.94×10^{-4}

Supporting Information 16:

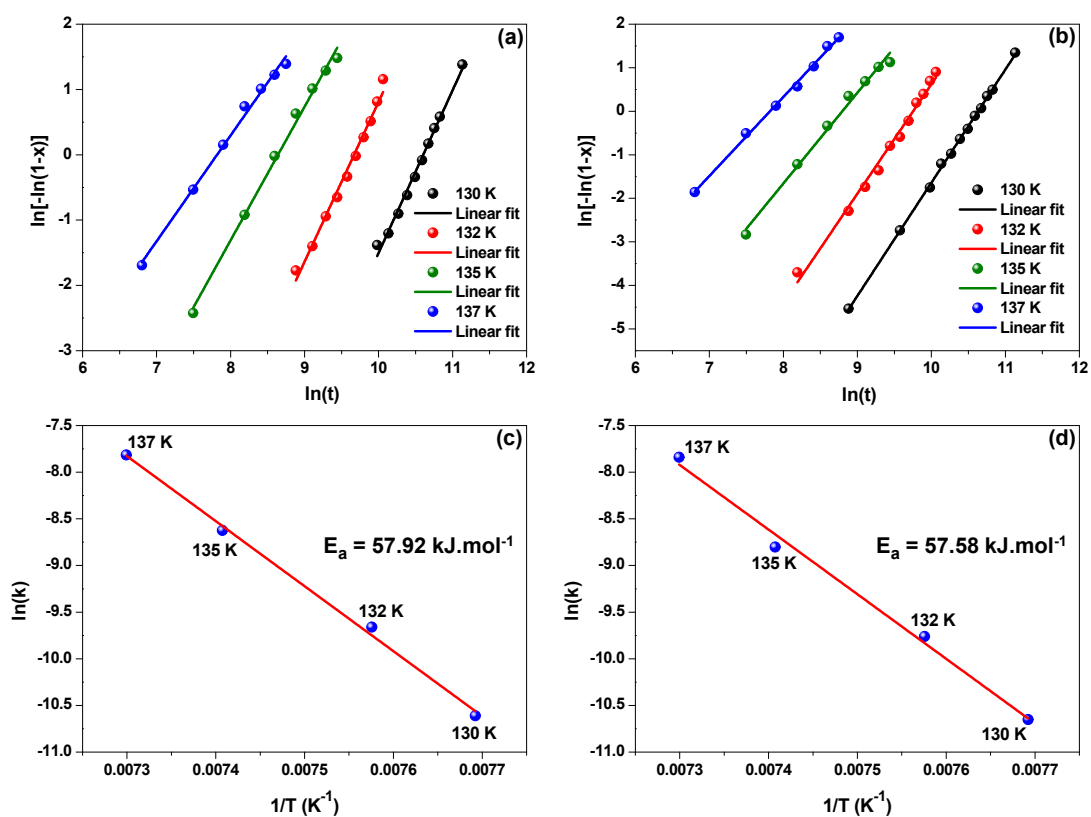


Figure S16. Plot of $\ln(-\ln[1-x(t)])$ vs. $\ln(t)$ at different temperatures of 130, 132, 135, and 137 K. These data points are obtained from the analysis of (a) the O-H, and (b) the O-D stretching regions and fitted using Avrami equation (eqn. 3). Plot of $\ln k(T)$ vs. inverse temperature ($1/T$), obtained from the analysis of (c) the O-H, and (d) the O-D stretching regions, respectively. The data points were fitted to obtain a straight line. Activation energy (E_a) can be calculated from the slope of the straight line.

References:

- (1) Bag, S.; Bhuin, R. G.; Methikkalam, R. R. J.; Pradeep, T.; Kephart, L.; Walker, J.; Kuchta, K.; Martin, D.; Wei, J.: Development of Ultralow Energy (1 - 10 eV) Ion Scattering Spectrometry Coupled with Reflection Absorption Infrared Spectroscopy and Temperature Programmed Desorption for the Investigation of Molecular Solids. *Rev. Sci. Instrum.* **2014**, *85*, 014103/1-014103/7.
- (2) Kim, Y.; Moon, E.-s.; Shin, S.; Kang, H.: Acidic Water Monolayer on Ruthenium(0001). *Angew. Chem., Int. Ed.* **2012**, *51*, 12806-12809.
- (3) Ghosh, J.; Hariharan, A. K.; Bhuin, R. G.; Methikkalam, R. R. J.; Pradeep, T.: Propane and propane-water interactions: a study at cryogenic temperatures. *Phys. Chem. Chem. Phys.* **2018**, *20*, 1838-1847.
- (4) Kang, H.; Shin, T. H.; Park, S. C.; Kim, I. K.; Han, S. J.: Acidity of Hydrogen Chloride on Ice. *J. Am. Chem. Soc.* **2000**, *122*, 9842-9843.
- (5) Bartmess, J. E.; Georgiadis, R. M.: Empirical methods for determination of ionization gauge relative sensitivities for different gases. *Vacuum* **1983**, *33*, 149-153.
- (6) Gottfried, J. M.; Schmidt, K. J.; Schroeder, S. L. M.; Christmann, K.: Oxygen chemisorption on Au(110)-(1×2) II. Spectroscopic and reactive thermal desorption measurements. *Surf. Sci.* **2003**, *525*, 197-206.
- (7) Yuan, C.; Smith, R. S.; Kay, B. D.: Communication: Distinguishing between bulk and interface-enhanced crystallization in nanoscale films of amorphous solid water. *J. Chem. Phys.* **2017**, *146*, 031102.
- (8) Li, F.; Skinner, J. L.: Infrared and Raman line shapes for ice Ih. II. H₂O and D₂O. *J. Chem. Phys.* **2010**, *133*, 244504.
- (9) Li, F.; Skinner, J. L.: Infrared and Raman line shapes for ice Ih. I. Dilute HOD in H₂O and D₂O. *J. Chem. Phys.* **2010**, *132*, 204505.
- (10) Souda, R.; Aizawa, T.: Crystallization kinetics of water on graphite. *Phys. Chem. Chem. Phys.* **2018**, *20*, 21856-21863.